Comparison of model and non-model based friction compensation techniques in the neighbourhood of pre-sliding friction

Vincent Lampaert, Jan Swevers, and Farid Al-Bender
Department of Mechanical Engineering, Division PMA
Katholieke Universiteit Leuven, Celestijnenlaan 300B, B3001 Belgium
jan.swevers@mech.kuleuven.ac.be

***Abstract*— This paper compares two different friction compensation techniques on a machine tool table: a friction model based feedforward technique and a disturbance observer which does not depend on a friction model. For the first technique, the performance of different friction models proposed in literature is compared. The disturbance observer estimates the friction force using a Kalman filter with a second order random walk model. Both approaches are complementary, yielding that their combination results in accurate tracking performance if the novel Generalized Maxwell-slip friction model is used.**

I. INTRODUCTION

Friction in mechanical systems is a nonlinear phenomenon which can cause control problems such as static errors, limit cycles and stick-slip. In order to design controllers for highly accurate machines, friction has to be compensated. Detailed analysis of friction experiments reveals two friction regimes: the pre-sliding regime and the sliding regime. In the pre-sliding regime the adhesive forces (at asperity contacts) are dominant such that the friction force appears to be a function of displacement rather than velocity. This is so because the asperity junctions deform elasto-plastically thus behaving as nonlinear hysteretic springs. As the displacement increases, more and more junctions will break resulting eventually in gross sliding. In the sliding regime all the asperity junctions are broken such that the friction force becomes also a function of the velocity in addition to the other states of the system [2].

This paper discusses the compensation of friction in pre-sliding regime only. A feedforward friction model based technique, using four different state-of-the-art models, and a non-model based technique, called disturbance observer, are described, implemented and compared experimentally on a machine tool table, which is an industrially relevant system. In order to use a compensation technique on a real industrial setup the following conditions have to be kept in mind: (i) the used technique should be stable, (ii) it should be easy to use in an existing control device, (iii) the computer memory needed for implementation should be as small as possible, and (iv) the computational cost must be as low as possible. Therefore the criteria of comparison are not only accuracy of compensation, but also stability, complexity of implementation (including parameter identification in case of the model based approaches) and computational cost.

The models that we selected for the feedforward compensation technique are some of the most effective ones given in the open literature: the Dahl model [4], the LuGre model [3], the Leuven model [12] [9], and the Generalized Maxwell-slip (GMS) friction model [7].

Section II discusses briefly the above mentioned friction models. Section III describes the machine tool table which is used to validated the different approaches. Section IV describes the friction-model-based feedforward compensation technique, its implementation for the different friction models, including the experimental identification of the model parameters, and the obtained results. Section V describes the disturbance observer its implementation and results. Section VI combines both techniques and shows the improved performance. Section VII formulates the concluding remarks.

II. FRICTION MODELS FOR CONTROL

This section briefly describes the four selected friction models.

A. The Dahl model

Dahl [4] developed a comparatively simple model which was used extensively to simulate systems with ball bearing friction and which has been used as a standard simulation model in aerospace industry. This friction model is an extension of Coulomb friction but it produces a smooth transition around zero velocity. The frictional hysteresis at pre-sliding is approximated by a generalized first order differential equation of the position depending only on the sign of the velocity v :

$$\frac{dF_f}{dx} = \sigma_0 \left| 1 - \frac{F_f}{F_s} \mathrm{sgn}\,(v) \right|^{\delta_d} \mathrm{sgn}\left(1 - \frac{F_f}{F_s} \mathrm{sgn}\,(v) \right) \quad (1)$$

with F_f the friction force, σ_0 the initial stiffness of the contact at velocity reversal, and F_s the static friction force. The exponent δ_d determines the shape of the hysteresis.

B. The LuGre model

A model which is in line with Dahl's considerations and employing the idea of an averaged deformation of the contact asperities has been developed at the universities of Lund and Grenoble [3] and is called the LuGre-model. It combines the pre-sliding behaviour of the Dahl model with the steady-state friction characteristic in sliding regime such

as the Stribeck curve $s(v)$. The friction force is given as a function of the state variable z and the velocity v:

$$F_f = \sigma_0 z + \sigma_1 \frac{dz}{dt} + \sigma_2 v. \tag{2}$$

where the parameters σ_0, σ_1 and σ_2 are the asperity stiffness, the micro-viscous friction coefficient and the viscous friction coefficient. The interpretation of the internal state is linked to the bristle friction model [6], viz. the state variable z represents the average deflection of the contacting asperities:

$$\frac{dz}{dt} = v - \sigma_0 \frac{v}{s(v)} z, \tag{3}$$

where $s(v)$, the Stribeck curve, is a decreasing function for increasing velocity bounded by an upper limit equal to the static force F_s and a lower limit equal to the Coulomb friction force F_c:

$$s(v) = \text{sgn}(v) \left(F_c + (F_s - F_c) e^{-|v/V_S|^{\delta_{V_S}}} \right), \tag{4}$$

with V_S the Stribeck velocity and δ_{V_S} the Stribeck shape factor.

C. The Leuven model

The Leuven model, presented by the authors [9], [12] was based on the experimental findings that the friction force in pre-sliding regime is a hysteresis function of the position, with non-local memory, which was only approximated by the former models. The Leuven model tries to fit this specific behavior into the LuGre-model in order to obtain better tracking results at velocity reversals [8]. The equations of the Leuven model are:

$$\frac{dz}{dt} = v \left(1 - \text{sgn} \left(\frac{F_h(z)}{s(v)} \right) \left| \frac{F_h(z)}{s(v)} \right|^{\delta_l} \right), \tag{5}$$

$$F_f = F_h(z) + \sigma_1 \frac{dz}{dt} + \sigma_2 v. \tag{6}$$

σ_1 and σ_2 have the same meaning as for the LuGre model. δ_l is the Leuven shape factor determining the transformation between the state variable z and the position x of the moving mass. The hysteresis function $F_h(z)$ can easily be implemented by using the Maxwell-Slip approximation [5],[9]. Its main advantages are the ease of implementation and the limited number of required memory. It consists of N elasto-plastic elements in parallel. Each element i has one common input z and one output F_i and each element is characterised by its own maximum elementary Coulomb force W_i, an elementary stiffness value k_i and a state variable ζ_i (see figure 1). The state variable ζ_i describes the position of element i. The elements have no mass, yielding a static relationship between the force F_i and the relative displacement $(z-\zeta_i)$ for each element. The relationship can be described as:

$$\text{if } |z-\zeta_i| < \tfrac{W_i}{k_i} \text{ then } \begin{cases} F_i = k_i (z-\zeta_i) \\ \zeta_i = \text{const.} \end{cases}$$

$$\text{else } \begin{cases} F_i = \text{sgn}(z-\zeta_i) W_i \\ \zeta_i = z - \text{sgn}(z-\zeta_i) \frac{W_i}{k_i} \end{cases}$$

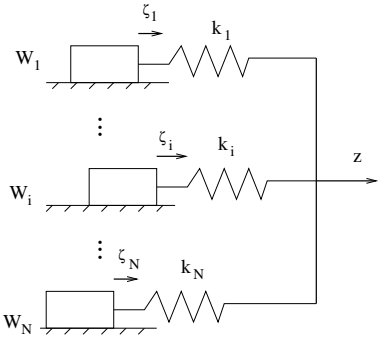

Fig. 1. Representation of the Maxwell-slip friction model using N elementary models.

The total hysteresis force is equal to the sum of hysteresis forces (F_i) of each element:

$$F_h(z) = \sum_{i=1}^{N} F_i(z). \tag{7}$$

D. The generalized Maxwell-Slip Friction Model

The generalized Maxwell-Slip (GMS) friction model [7] is developed from a physically motivated friction model [1] and is based explicitly on three friction properties: (i) the Stribeck curve for constant velocities, (ii) the hysteresis function with non-local memory in the pre-sliding regime, and (iii) the frictional memory in the sliding regime. The developed model is a parallel connection of different single state friction models, all having the same input namely the velocity v. The friction force is given as the summation of the outputs of the N elementary state models plus an extra viscous term, if viscous friction is present at the interface:

$$F_f(t) = \sum_{i=1}^{N} F_i(t) + \sigma_2 v(t).$$

The dynamic behavior of each elementary model i can be written as:

- If the elementary model is sticking, the state equation is given by:

  $$\frac{dF_i}{dt} = k_i v.$$

  The elementary model remains sticking until $F_i > \alpha_i s(v)$ ($\alpha_i = const$).
- If the elementary model is slipping, the state equation is given by:

  $$\frac{dF_i}{dt} = \text{sgn}(v) C \left(\alpha_i - \frac{F_i}{s(v)} \right).$$

  The elementary model remains slipping until the velocity goes through zero.

The parameter σ_2 and the Stribeck curve $s(v)$ are the same as for the LuGre and Leuven model. The attraction parameter C determines the attraction of the total friction force towards the Stribeck curve in sliding. Each elementary model i has its own elementary stiffness k_i, and elementary

fractional parameter α_i. This latter determines the maximal force for each F_i during sticking.

Further details of these models can be found in the mentioned references. The identification of the model parameters is discussed in section IV.

III. MACHINE TOOL TABLE SYSTEM

Figure 2 shows the machine tool table system used to validate experimentally the friction models. The table is guided and supported by two recirculating-roller guideways each with two carriages. All the bearings in the system are of rolling-element type. A 50-mm pitch-size ball-screw couples the table to a screw which is directly connected to the rotor of a brushless permanent magnet servo motor (Parvex LD840EE) by a stiff coupling without any reduction.

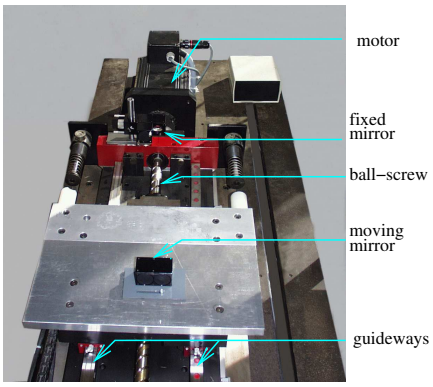

Fig. 2. The machine tool table setup used to validate experimentally the tracking performance for sliding trajectories. The motor (top of the figure) is directly connected to the screw which is coupled to the table (bottom of the figure) via a ball-screw.

A Renishaw interferometer with a resolution of 10 nm measures the position of the table by measuring the relative distance between two mirrors, one attached to the frame, the other attached to the table. The control input to the system is a voltage between $\pm$ 10 Volt which is converted by the motor's current amplifier (Parvex AMS2) into a current signal. This current signal is proportional to the applied force to the rotor. The friction force itself is not directly measurable. However, after compensation the cogging force and for small accelerations of the table, the friction force corresponds to the applied force and can thus be derived therefrom.

The cogging force is a magnetic disturbance force. It is the force needed to keep the rotor at a certain position due to the magnets and depends only on the position of the rotor with respect to the stator. The cogging force is identified using the technique described in [13]. It has been modelled using a finite Fourier series and compensated by means of table position-driven feedback.

The different friction compensation techniques, discussed below, are tested in combination with a weak PD feedback controller. Without feedback controller, the machine tool table will drift. A weak controller is selected in order to clearly see the influence of the compensation techniques.

To investigate the tracking performance in pre-sliding regime, a desired position signal as shown in figure 3A is applied to the system. This pre-sliding trajectory is chosen such that a large range of the pre-sliding regime is covered and two inner hysteresis loops are made during one reference period. With this signal it is possible to investigate the influence of the nonlocal memory on the tracking behavior. The resulting peak-to-peak position error for the feedback controller only equals 46.2 μm.

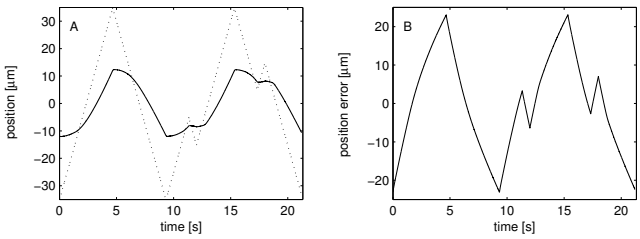

Fig. 3. Experimental results on the machine tool table using a simple feedback controller. Fig. A: the desired (dashed line) and real (full line) position as a function of time. Fig. B: the position error as a function of time.

IV. FEEDFORWARD FRICTION-MODEL-BASED COMPENSATION

This section discusses feedforward friction-model-based compensation using the four friction models discussed in section II. The applied force to the system corresponds to the sum of the output u of the feedback controller and the estimated friction force $\hat{F}_f$:

$$F_a = u(t) + \hat{F}_f(x_d, \frac{dx_d}{dt}),$$

where x_d represents the desired position trajectory.

The parameters of the different friction models have to be identified. This is a nonlinear parameter identification problem, consisting of different steps and dedicated experiments, as described in the following paragraph.

A. Friction model parameter identification

The Stribeck curve (Eq. 4), used by the LuGre, Leuven, and GMS model, can be identified by imposing on the system different constant velocities and using a nonlinear least-squares curve-fitting techniques. Figure 4 shows the measured and estimated Stribeck curve. The estimated parameters are $F_s = 54\ N$, $F_c = 39.2\ N$, $\delta_{V_S} = 0.98$, $V_S = 698\ \mu m/s$, and $\sigma_2 = 8.4e-5\ Ns/\mu m$.

In order to identify the pre-sliding regime parameters a low-velocity saw-signal is imposed to the system using a stiff PID-controller. Figure 4B shows the measured and identified hysteresis shape for the Maxwell-slip model with 12 elements, using standard linear least squares techniques. The estimated Dahl parameters, $\delta_d = 5.14$ and $\sigma_0 = 1.4N/\mu m$, are estimated using a nonlinear curve-fitting technique.

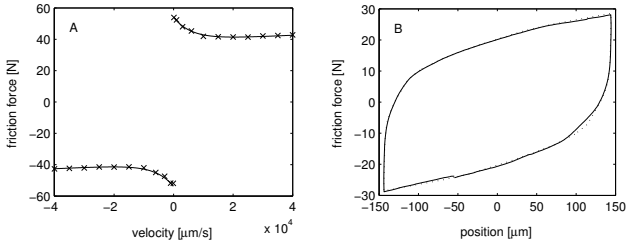

Fig. 4. Figure A: the crosses correspond to the measured friction force values for different steady-state velocities. The full line is the estimated Stribeck curve. Figure B: The full line corresponds to a measured hysteresis curve of the friction force in pre-sliding regime. The dotted line corresponds to the estimated curve using elementary Maxwell-Slip models.

	memory	+	x	exp	pow
Dahl	8	4	8	1	2
LuGre	8	6	9	1	1
Leuven	$8+3N$	$6+2N$	$9+2N$	1	2
GMS	$6+4N$	$2+3N$	$2+10N$	1	1

TABLE I

REQUIRED PARAMETER COMPUTER MEMORY AND COMPUTATIONAL COST NECESSARY TO APPLY THE FRICTION-MODEL-BASED FEEDFORWARD COMPENSATION TECHNIQUE.

The remaining three parameters are hand-tuned to minimize the maximum position error for the given trajectory, yielding: $C = 65\ N/s$, $\delta_l = 0.1$, and $\sigma_1 = 0.01\ Ns/\mu m$.

Table I shows, for the considered friction models, the computer memory required to store the model parameters and variables and computational cost for one model evaluation. N is the number of used elementary (Generalized) Maxwell-slip models in the Leuven and GMS model.

B. Compensation results for the machine tool table

Figure 5A shows the position error using the feedback controller and the Dahl model as feedforward model. The error using the Dahl model is smaller than the error using the LuGre model (figure 5B). This is due to the fact that the Dahl model offers more flexibility (by the shape factor δ_d) than the LuGre model to model the pre-sliding hysteresis curve.

The GMS model gives best results (figure 5D), better than the Leuven model (figure 5C), although the Leuven model uses a Maxwell-slip model to approximate the hysteresis function. This is a result of the nonlinear transformation between the z-variable (Eq. 5), which is the real input to the Maxwell-slip model in the Leuven model, and the position x which has been used to identify the Maxwell-slip model. As a result of this transformation the friction force in pre-sliding will be a deformed hysteresis curve. Figure 6 shows the estimated friction force as a function of the desired position signal for the different used friction models. A better way to identify the parameters of the Maxwell-slip model in the Leuven model, is first to convert the position signal into the z-variable and then perform the Maxwell-slip model parameter identification. This approach is however not straightforward, since the nonlinear transformation depends on the hysteresis curve.

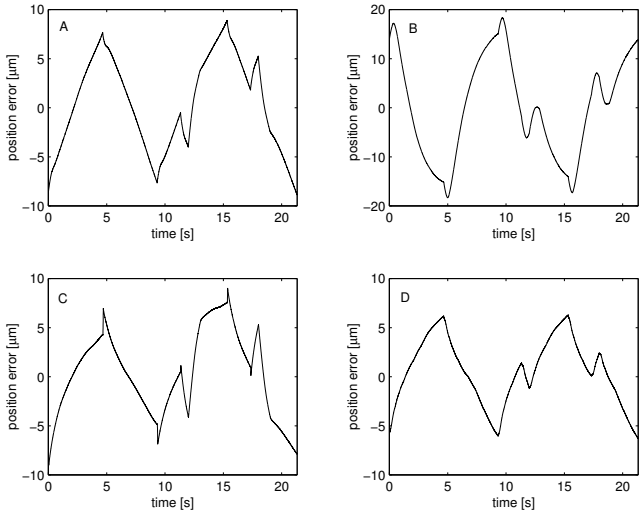

Fig. 5. The position error as a function of time: (A)Dahl model, (B)LuGre model, (C)Leuven model, (D)GMS model.

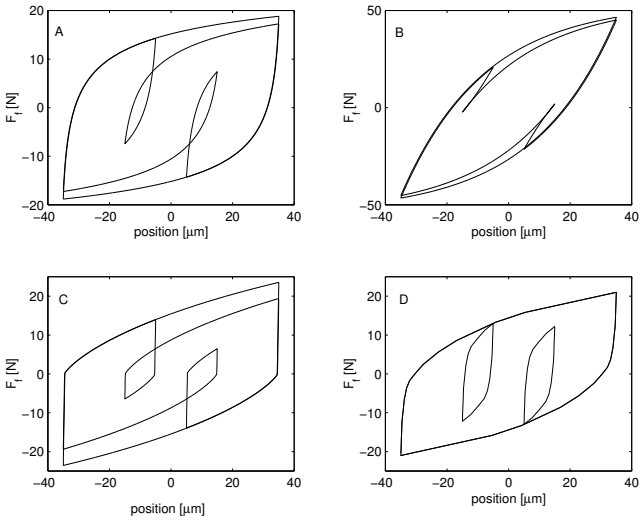

Fig. 6. The estimated friction force as a function of the desired position: (A)Dahl model, (B)LuGre model, (C)Leuven model, (D)GMS model.

Despite the accuracy of the Maxwell-Slip model used in the GMS model, the tracking error remains relatively large. This is due to the fact that the friction force compensation uses the desired position instead of the real position signal, which is lagging behind due to the weak feedback controller. Friction-model-based feedback compensation is not attempted here to avoid instability problems.

V. DISTURBANCE OBSERVER

This section discusses the use of the disturbance observer technique to compensate friction, where the applied force to the system equals:

$$F_a = u(t) + \hat{F}_{dist}\left(x, F_a\right),$$

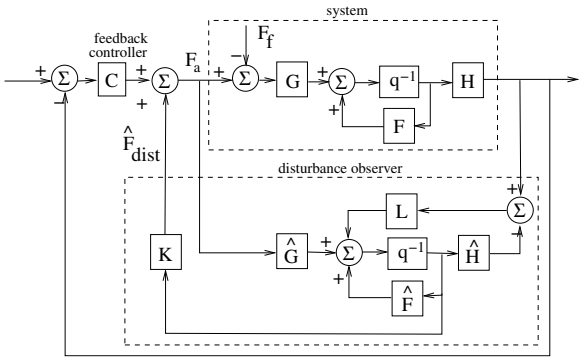

Fig. 7. The general scheme for a discrete disturbance estimator.

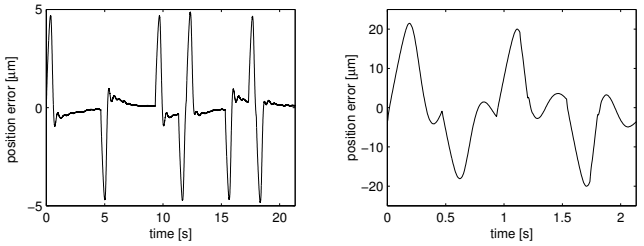

Fig. 8. The position error as a function of time using a disturbance observer. Fig A: the position error for the reference pre-sliding trajectory. Fig. B: the position error for the reference pre-sliding trajectory executed ten times faster.

with $\hat{F}_{dist}$ the output of the disturbance observer. Different types of disturbance observers exist. This paper considers the approach proposed by Ray *et al.* [11]. The basic idea behind it is the following: by measuring motion along with applied force F_a, and knowing the system dynamic model, one can estimate the external friction force using an observer as shown in figure 7. Kalman filter techniques can be used to design this observer. Ray *et al.* [11] model the friction force as an n-th order random walk. This paper considers a disturbance observer based on a second order random walk. The state vector of the system is $X = \left[\begin{array}{cc} v(k) & x(k) \end{array} \right]^T$ and the system matrices (see figure 7) describing the system dynamics, are:

$$F = \left[\begin{array}{cc} 1 - \sigma_2 T_s/M & 0 \\ Ts & 1 \end{array} \right], G = \left[\begin{array}{c} T_s/M \\ 0 \end{array} \right], H = \left[\begin{array}{cc} 0 & 1 \end{array} \right].$$

The state vector of the observer equals $\hat{X} = \left[\begin{array}{cccc} \hat{v}(k) & \hat{x}(k) & \hat{F}_f(k) & d\hat{F}_f(k) \end{array} \right]^T$ and the matrices representing the observer dynamics are:

$$\begin{aligned} \hat{F} &= \left[\begin{array}{cccc} 1 - \hat{\sigma}_2 T_s/\hat{M} & 0 & -T_s/\hat{M} & 0 \\ T_s & 1 & 0 & 0 \\ 0 & 0 & 1 & T_s \\ 0 & 0 & 0 & 1 \end{array} \right], \\ \hat{G} &= \left[\begin{array}{c} T_s/\hat{M} \\ 0 \\ 0 \\ 0 \end{array} \right], \quad \hat{H} = \left[\begin{array}{cccc} 0 & 1 & 0 & 0 \end{array} \right], \\ K &= \left[\begin{array}{cccc} 0 & 0 & 1 & 0 \end{array} \right], \end{aligned}$$

and L is the observer gain vector, which is tuned by considering the following trade-off: fast response, minimal overshoot, low-noise sensitivity, and robustly stable behavior.

Fifteen floating point variables/parameters are required to implement this disturbance observer, and the computational cost equals 10 summations and 15 multiplications in case of fixed observer gains.

Figure 8A shows the tracking error for the specified trajectory. The maximum error (peak-to-peak error equals 9.7 μm) is comparable with the best feedforward friction compensation results. These good results are due to the fact that the disturbance observer not only compensates the friction disturbance, but also the error due to the weakly tuned PD-controller. However, for faster reference trajectories, the position error increases (see figure 8B) because the disturbance observer has a limited disturbance rejection bandwidth.

VI. Feedforward friction compensation in combination with a disturbance observer

This section combines the techniques of the previous two sections. A similar combination is described in Lee and Tomizuka [10], using static friction model. The input of the disturbance observer is now the difference between the applied force and the estimated friction force instead of the applied force only:

$$F_a = u(t) + \hat{F}_f(x_d, \frac{dx_d}{dt}) + \hat{F}_{dist}\left(x, F_a - \hat{F}_f\right).$$

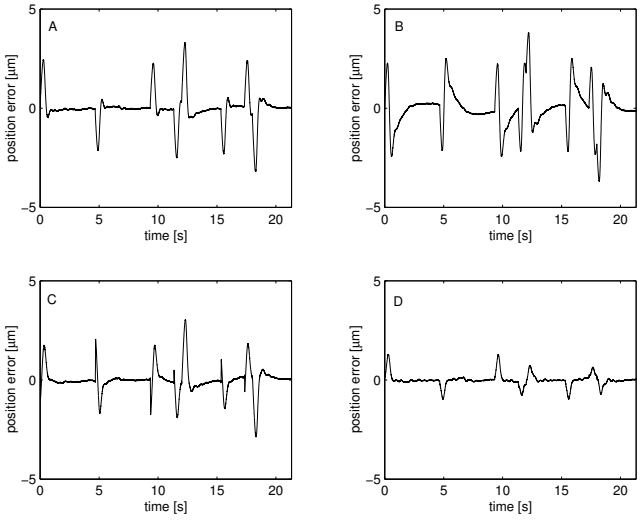

Fig. 9. The pre-sliding tracking performance using a disturbance observer and a feedforward friction-model-based compensator. The position error as a function of time using the Dahl model (fig. A), the LuGre model (fig. B), the Leuven model (fig. C), and the GMS model (fig. D).

Figure 9 shows the tracking error for the different friction models in feedforward. The peak-to-peak position errors are

$6.6\ \mu m$, $7.6\ \mu m$, $6.1\ \mu m$, and $2.6\ \mu m$, using the Dahl, LuGre, Leuven, and GMS friction model, respectively. The tracking error is reduced significantly for all the friction models. The best results are obtained using the GMS friction model.

This significant reduction of the tracking error indicates that both techniques are complementary to each other. The disturbance observer is able to compensate arbitrary disturbances up to a limited bandwidth. It reduces the tracking error in general, but is not able to compensate for fast friction force changes at velocity reversal. The feedforward technique can compensate these fast friction force changes provided that the tracking error is already small, which can be accomplished using the disturbance observer, and provided that the friction model is accurate. The recently developed Generalized Maxwell-slip friction model [7] yields the best results.

VII. Conclusions

Combining a friction-model-based feedforward compensation and a disturbance observer yields many advantages with respect to the individual techniques. Firstly, a significant improvement of the pre-sliding tracking accuracy is achieved, which is mainly because both techniques complement each other. Secondly, stability is not compromised in order to get this level of accuracy. This is because the bandwidth of the disturbance observer does not have to be pushed to the limit in order to compensate fast friction changes since these are taken care of by the feedforward part, which is inherently stable. Thirdly, the disturbance observer increases the robustness against model parameter changes.

The GMS friction model yields significantly better tracking results than the other presented models, while its computational cost and the complexity of its parameter identification are comparable with the others.

ACKNOWLEDGMENTS: This paper presents research results of the Belgian programme on Interuniversity Poles of attraction by the Belgian State, Prime Minister's Office, Science Policy Programming. K.U.Leuven's Concerted Research Action GOA/99/04 is gratefully acknowledged. The scientific responsibility is assumed by its authors.

References

[1] F. Al-Bender, V. Lampaert, and J. Swevers, *A novel generic model at asperity level for dry friction force dynamics*, accepted for Tribology Letters (2003).

[2] B. Armstrong-Hélouvry, *Control of machines with friction*, Kluwer Acacemic Publishers, 1991.

[3] C. Canudas de Wit, H. Olsson, K. Aström, and P. Lischinsky, *A new model for control of systems with friction*, IEEE Transactions on Automatic Control **40** (1995), no. 5, 419–425.

[4] P.R. Dahl, *A solid friction model*, The Aerospace Corporation, El Segundo, CA, TOR-158(3107-18), 1968.

[5] W. D. Iwan, *A distributed-element model for hysteresis and its steady-state dynamic response*, Transactions of the ASME, Journal of Aplied Mechanics **33** (1966), no. 4, 893–900.

[6] D. Karnopp, *Computer simulation of slip-stick friction in mechanical dynamic systems*, Trans. of the ASME, Journal of Dynamic Systems, Measurement, and Control **107** (1985), no. 1, 100–103.

[7] V. Lampaert, F. Al-Bender, and J. Swevers, *A generalized maxwell-slip friction model appropriate for control purposes*, Proc. of the IEEE int. conf. Physics and Control (Saint-Petersburg) **CD-rom** (2003).

[8] V. Lampaert, J. Swevers, and F. Al-Bender, *Experimental comparison of different friction models for accurate low-velocity tracking*, Proc. of the Med. Conf. on Control and Automation (Lisbon) (2002).

[9] ———, *Modification of the leuven integrated friction model structure*, IEEE Transactions on Automatic Control **47** (2002), no. 4, 683–687.

[10] H. S. Lee and M. Tomisuka, *Robust motion controller design for high-accuracy positioning systems*, IEEE Trans. on Ind. Electronics **43** (1996), no. 1.

[11] L.R. Ray, A. Ramasubramanian, and J. Townsend, *Adaptive friction compensation using extended kalman-bucy filter friction estimation*, Control Engineering Practice **9** (2001), 169–179.

[12] J. Swevers, F. Al-Bender, C. Ganseman, and T. Prajogo, *An integrated friction model structure with improved presliding behaviour for accurate friction compensation*, IEEE, trans. on Automatic Control **45** (2000), no. 4, 675–686.

[13] P. Van de Braembussche, J. Swevers, H. Van Brussel, and P. Vanherck, *Accurate tracking control of linear synchronous motor machine tool axes*, Mechatronics **6** (1996), no. 5, 507–521.